

Modelling the Impacts of Shape and Volume Fraction of Nanoparticles on Water Based Nanofluid Flow with Variable Thermophysical Properties

C. Nwaigwe^{1*}, A. Weli², F. Mebarek-Oudina³

^{1,2} Department of Mathematics, Rivers State University, Port Harcourt, Nigeria.

³ Department of Physics, Faculty of Sciences, University of 20 Août 1955-Skikda, Skikda, Algeria.

^{1,*} Corresponding author: nwaigwe.chinedu@ust.edu.ng

² weli.azubuike@ust.edu.ng, ³ oudina2003@yahoo.fr

Article Info

Received: 01 March 2023 Revised: 22 March 2023

Accepted: 24 March 2023 Available online: 28 March 2023

Abstract

In some applications, nano-sized particles are used to enhance heat transfer in thermal energy systems. Two important practical concerns are the shape of the nanoparticles and the volume fraction that could lead to optimal performance. This study investigates the effects which the shape and volume fraction of copper nanoparticles may have on the velocity and temperature of water based nanofluid. To account for more physical reality, we incorporate the variability of the viscosity and thermal conductivity. The Hamilton-Crosser's model of nanofluid thermal conductivity is also adopted. It is proposed that for a fluid with temperature-dependent thermo-physical properties, the fluid thermal conductivity in the Hamilton-Crosser's relation should be replaced with a constant (temperature-independent) thermal conductivity. The governing system of nonlinear partial differential equations is solved by using a convergent finite difference scheme. The results show that increasing the volume fraction decreases the velocity but increases the temperature, while copper nanoparticles of spherical shape lead to enhanced temperature than other shapes.

Keywords: Nonlinear suction velocity; Variable viscosity; Variable thermal conductivity; Hamilton-Crosser Relation; Implicit-explicit finite difference scheme. .

MSC2010: 76D05, 76D07, 76N10.

| | | | |
|----------------|--|-----------------|--|
| u | Nanofluid velocity (dimensional). | U_0 | Free stream velocity. |
| T | Nanofluid temperature (dimensional). | T_∞ | Ambient temperature. |
| μ_0 | Water viscosity at constant temperature. | κ_0 | Thermal conductivity of Water at constant temperature. |
| H_m | Channel width (dimensional). | $\tilde{\beta}$ | Thermal conductivity variation parameter. |
| T_w | Wall Temperature (dimensional). | P_r | Prandtl number. |
| κ_f | Variable thermal conductivity of water. | κ_p | Thermal conductivity of copper. |
| μ_f | Variable viscosity of water. | ϕ | Volume fraction of copper nanoparticles. |
| $(\rho C_p)_f$ | Heat Capacity of water. | $(\rho C_p)_p$ | Heat Capacity of copper. |
| ρ_f | Density of water. | ρ_p | Density of copper. |
| $\rho_{n,f}$ | Density of water-copper nanofluid. | n_p | Shape factor of nanoparticles. |
| $\kappa_{n,f}$ | Thermal conductivity of nanofluid. | $\sigma_{n,f}$ | Electrical conductivity. |
| B | Magnetic Field constant. | $\beta_{Tn,f}$ | Thermal expansivity. |
| w_* | Constant velocity. | α | viscosity parameter. |
| λ | Wall suction parameter. | $\bar{\alpha}$ | Viscosity variation parameter. |
| g | acceleration due to gravity. | | |
| β | Thermal conductivity parameter. | | |
| H^2 | Hartman number. | | |
| G_r | Grashof number. | | |
| Q_s | Heat source parameter. | | |
| θ | nondimensional temperature. | | |
| y, t | non-dimensional space variable, time variable. | | |

1 Introduction

One innovative approach to optimize the performance of thermal energy systems is the suspension of metallic nanometer-sized particles in a base fluid such as water, oil, ethylene, biofluids and lubricants. Such suspension of nanoparticles in a base fluid is called a nanofluid, and it can improve the thermo-physical properties of the base fluid [1]. The term nanofluid was first coined by Choi [2] who applied some nanoparticles into a base fluid to enhance thermal conductivity. Nanofluids find applications in diverse areas, including biomedical engineering, nuclear reactors, cooling systems, solar energy systems, and automobile and IT industries [1–3].

The numerous applications mentioned above have attracted much research in nanofluids and nanotechnology. For example, [4] investigated the heat transfer in a steady flow of water-copper nanotubes in a backward-facing channel, while [5] considered the pressure drop and heat transfer in a water based nanofluid flow in a heat exchanger. The influence of variable heat source on MHD nanofluid flow over a stretchable disk with double-diffusion is investigated in [6]. The comparative analysis of two nanofluids, namely water-aluminum oxide and water-copper oxide, is undertaken in [7]. Constant thermo-physical properties are considered. Their resulting partial differential equations were solved using the method of Laplace transform. It is found that an increase in the Hartmann number increases the flow of copper oxide nanofluid compared to the aluminum nanofluid. Other investigations include those of [8,9] and a review on the combined use of porous media and nanofluids to optimize heat transfer can be found in [10].

Recently, [11] investigated heat transfer in an unsteady nanofluid flow over a rotating plate, accounting for viscous dissipation, and Brownian and thermophoresis diffusion. The base fluid is water and three nanoparticles were considered, namely copper, aluminum oxide and titanium dioxide. They assumed all thermophysical properties to be constant and the formulated model was solved using the homotopy perturbation method. Their results show that the shape of nanoparticles has an influence on the rate of heat transfer. It is well known that real fluid properties are, in general, not constant, they vary with temperature [1]. In this line, a comparison of the results obtained from making constant property assumptions and variable property assumptions was undertaken in [12]. The variable properties were assumed to depend on temperature. It was found that constant property assumptions do not lead to correct prediction of flow and heat transfer processes. This is especially important when the temperature variations are significant. Hence, it is important to consider thermo-physical properties as non-constants.

Consequently, [1] investigated the effects of variations in the effective viscosity of water-based nanofluids. The variability of the viscosity with temperature is assumed to be linear and the thermal conductivity was still assumed to be constant. Their results show that increasing the variable

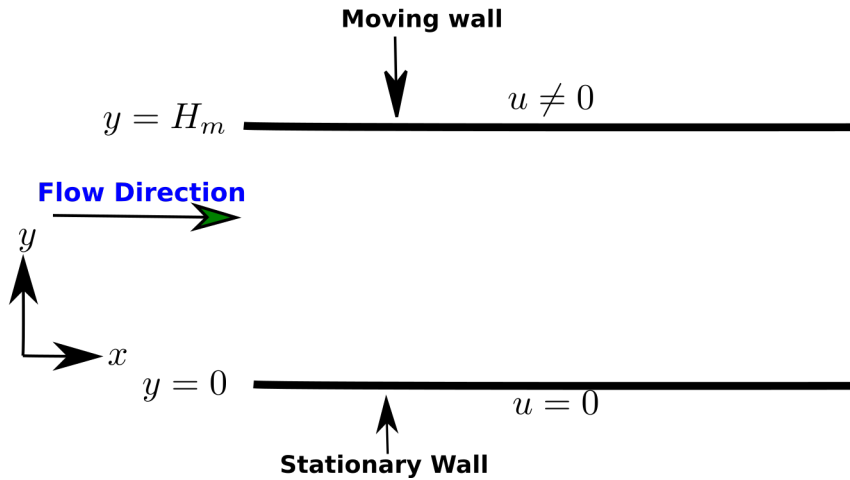


Figure 1: Physical set up

viscosity parameter led to increased velocity. See also [13] for a related study. As mentioned above, it is important to consider variable properties, however their work of [1] only considered the case of linear variation in viscosity, yet allowed the thermal conductivity to remain constant. Again, their work does not consider time evolution of the flow, it considered only a steady flow, just like those of [7]. This is a gap that the current study fills. The present study aims to extend the works of [1] by accounting for unsteadiness, and nonlinearly variable viscosity and thermal conductivity. We also incorporate nonlinear wall suction velocity, this aspect is an extension of the work of [11]. This study is significant as it helps to understand flow and temperature variations of a nanofluid consisting of a base fluid with temperature-dependent properties. The objectives of the present work is to answer the following questions:

1. what is the effect of variable viscosity on the flow?
2. what is the effect of suction velocity on the flow?
3. what is the effect of variable thermal conductivity?
4. how does the shape of nanoparticles affect the flow?
5. how does the volume fraction of the nanoparticles affect the flow?

In section 2, we present the assumptions on the problem and the constitutive relations, then formulate the governing equations for the problem. In section 3 we formulate a numerical method for solving the proposed mathematical model. The investigation of the effects of the various parameters on the velocity and temperature profiles are given in section 4, while conclusions are made in section 5.

2 Mathematical Formulation of the Problem

We consider the unsteady flow of a nanofluid consisting of copper nanoparticles and water in a rectangular channel, see Figure 1. The coordinate axes (x, y, z) is chosen such that the x -axis is along the channel, the y -axis is perpendicular to the x -axis and along the lateral (width) direction of the channel, while the z -axis is vertically upwards and perpendicular to the $x - y$ plane. The ambient temperature and free stream velocity are T_∞ and U_0 respectively.

Fluid properties are generally not constant [1], hence we consider water as an incompressible base fluid with variable thermo-physical properties. However, we require that at constant temperature, the values of the thermo-physical properties must coincide with those of their temperature-independent values. To achieve this, we model water as a fluid with temperature-dependent viscosity and thermal conductivity [14–16] given by

$$\mu_f(T) = \mu_0 e^{-\bar{\alpha}(T-T_\infty)}$$

and

$$\kappa_f(T) = \kappa_0 e^{\bar{\beta}(T-T_\infty)}$$

respectively, where μ_0 and κ_0 are constant viscosity and thermal conductivity of water, respectively, $\bar{\alpha}$, $\bar{\beta}$ are positive constants, T_w is the temperature at the channel wall, and T is a variable representing the temperature. Notice that when $T = T_\infty$ both μ_f and κ_f reduce to their constant values, μ_0 and κ_0 respectively.

The copper nanoparticles have constant properties with constant thermal conductivity, κ_p . The particle-fluid solution is a homogeneous mixture without slip. The effective viscosity of the nanofluid is given by the Brinkman's [17] viscosity model in the case of two phase flow:

$$\mu_{nf}(T) = \frac{\mu_f(T)}{(1-\phi)^{2.5}}, \quad (2.1)$$

where ϕ is the nanoparticle's volume fraction. Let ρ_p , ρ_f denote the nanoparticle and fluid (water) densities, respectively and $(\rho C_p)_p$, $(\rho C_p)_f$ their constant heat capacities. Then the effective density and heat capacity of the nanofluid are given by

$$\rho_{nf} = (1-\phi)\rho_f + \phi\rho_p \quad (2.2)$$

and

$$(\rho C_p)_{nf} = (1-\phi)(\rho C_p)_f + \phi(\rho C_p)_p \quad (2.3)$$

respectively [18,19].

To account for the effects of the shape of nanoparticles, we employ the Hamilton-Crosser's model [20] which states that the effective thermal conductivity of the nanofluid satisfies:

$$\frac{\kappa_{nf}}{\kappa_f} = \frac{\kappa_p + (n_p - 1)\kappa_f - (n_p - 1)\phi(\kappa_f - \kappa_p)}{\kappa_p + (n_p - 1)\kappa_f + \phi(\kappa_f - \kappa_p)}, \quad (2.4)$$

where n_p indicates the shape factor of the nanoparticles, and is given by

$$n_p = \begin{cases} 3, & \text{for spherical nanoparticles,} \\ 6, & \text{for cylindrical nanoparticles,} \\ 3.7, & \text{for brick-shaped nanoparticles.} \end{cases}$$

However, in this work, we propose that if a base fluid has a temperature-dependent thermal conductivity κ_f , and a temperature-independent thermal conductivity κ_0 , then κ_f in the Hamilton-Crosser's relation (2.4) should be replaced with the constant value, κ_0 . That is, we have:

$$\frac{\kappa_{nf}}{\kappa_f} = \frac{\kappa_p + (n_p - 1)\kappa_0 - (n_p - 1)\phi(\kappa_0 - \kappa_p)}{\kappa_p + (n_p - 1)\kappa_0 + \phi(\kappa_0 - \kappa_p)}. \quad (2.5)$$

We further assume that the flow is dominated along the x -axis, fully developed and with no slip on the channel walls. One of the channel walls is permanently at rest while the other moves with time-dependent velocity. Also, the channel wall is porous and suction (draining) is significant and depends nonlinearly on the velocity. Constant magnetic field is applied and buoyancy forces

due to thermal energy is significant. The wall temperatures are kept constant and a linear heat source is applied. With these assumption, the continuity equation asserts that the fluid velocity is independent of both x and z directions, the same is true for the temperature. Hence, the equations governing the velocity, $u(y, t)$ and temperature, $T(y, t)$ of the nanofluid at time t , position, y , are the following [21–24]:

$$\rho_{nf} \left(\frac{\partial u}{\partial t} + w_0(u) \frac{\partial u}{\partial y} \right) = \frac{\partial}{\partial y} \left(\mu_{nf}(T) \frac{\partial u}{\partial y} \right) - \sigma_{nf} B^2 u + \rho_{nf} B_{Tnf} g(T - T_\infty), \quad y \in (0, H_m) \quad (2.6)$$

$$(\rho C_p)_{nf} \left(\frac{\partial T}{\partial t} + w_0(u) \frac{\partial T}{\partial y} \right) = \frac{\partial}{\partial y} \left(\kappa_{nf}(T) \frac{\partial T}{\partial y} \right) + Q(T - T_\infty), \quad y \in (0, H_m) \quad (2.7)$$

where σ_{nf} , B , β_{Tnf} and Q are the electric conductivity, magnetic field constant, thermal expansivity and heat source constant, while $w(u) = w_* e^{\bar{c}u}$ is the suction (wall draining) velocity, w_* is a constant velocity and $H_m = \frac{\mu_0}{U_0 \rho_f}$ is the channel width. The boundary and initial conditions are

$$\begin{aligned} u(0, t) = 0, u(H_m, t) = U_0 e^{tU_0^2 \rho_f / \mu_0} \quad \text{for all } t \geq 0, \\ T(0, t) = T(H_m, t) = 0.5(T_w - T_\infty) + T_\infty, \quad \text{for all } t \geq 0, \\ u(y, 0) = U_0 (U_0 \rho_f / \mu_0)^2 y^2, \quad T(y, 0) = 0.5(T_w - T_\infty) + T_\infty \quad y \in [0, H_m]. \end{aligned} \quad (2.8)$$

The nondimensional form of the model is presented next.

2.1 Nondimensionalization

To derive the nondimensional forms of the equations, we define the following nondimensional quantities:

$$\begin{aligned} (\bar{x}, \bar{y}) &= \frac{(x, y)U_0}{\mu_0} \rho_f, \quad \bar{t} = \frac{U_0^2 t \rho_f}{\mu_0}, \quad \bar{u} = \frac{u}{U_0}, \quad \theta = \frac{T - T_\infty}{T_w - T_\infty}, \\ H^2 &= \frac{B^2 \mu_0 \sigma_f}{\rho_f^2 U_0^2}, \quad G_r = \frac{\mu_0 g (T_w - T_\infty)}{\rho_f U_0^3}, \quad P_r = \frac{\mu_0 C_{p,f}}{\kappa_0}, \\ Q_s &= \frac{Q \mu_0}{U_0^2 \rho_f (\rho C_p)_{nf}}. \end{aligned} \quad (2.9)$$

Using the above nondimensional quantities, equation (2.6) becomes:

$$\begin{aligned} \frac{U_0^3 \rho_f}{\mu_0} \frac{\partial \bar{u}}{\partial \bar{t}} + \frac{U_0^2 \rho_f}{\mu_0} w_0(u) \frac{\partial \bar{u}}{\partial \bar{y}} &= \frac{U_0^3 \mu_0 \rho_f^2}{\mu_0^2 (1 - \phi)^{2.5} \rho_{nf}} \frac{\partial}{\partial \bar{y}} \left(e^{-\alpha \theta} \frac{\partial \bar{u}}{\partial \bar{y}} \right) - \frac{\sigma_{nf} B^2 U_0 \bar{u}}{\rho_{nf}} \\ &\quad + \beta_{Tnf} g (T_w - T_\infty) \theta \\ \Rightarrow \frac{\partial \bar{u}}{\partial \bar{t}} + \frac{w_0(u)}{U_0} \frac{\partial \bar{u}}{\partial \bar{y}} &= - \frac{\mu_0}{U_0^3 \rho_f \rho_{nf}} \frac{\partial p}{\partial x} + \frac{\rho_f}{\rho_{nf} (1 - \phi)^{2.5}} \frac{\partial}{\partial \bar{y}} \left(e^{-\alpha \theta} \frac{\partial \bar{u}}{\partial \bar{y}} \right) - \frac{\sigma_{nf} B^2 \mu_0 \bar{u}}{u_0^2 \rho_f \rho_{nf}} \\ &\quad + B_{Tnf} \frac{\mu_0 g (T_w - T_w)}{u_0^3 \rho_f} \theta \\ &= \frac{A_1}{(1 - \phi)^{2.5}} \frac{\partial}{\partial \bar{y}} \left(e^{-\alpha \theta} \frac{\partial \bar{u}}{\partial \bar{y}} \right) - A_1 A_3 H^2 \bar{u} + A_1 A_4 G_r \theta \end{aligned}$$

Because

$$\frac{\sigma_{nf} B^2 \mu_0}{u_0^2 \rho_f \rho_{nf}} = \frac{\sigma_{nf}}{\sigma_f} \frac{B^2 \mu_0 \sigma_f}{\rho_f^2 u_0^2} \frac{\rho_f}{\rho_{nf}} = J_3 H^2 J_1,$$

and

$$\begin{aligned} \frac{\mu_0 g(T_w - T_\infty)}{u_0^3 \rho_f} \beta_{T_{nf}} &= \frac{\mu g(T_w - T_\infty)}{\rho_f u_0^3} \beta_{T_f} \frac{\beta_{T_{nf}}}{\beta_{T_f}} = G_r \frac{\beta_{T_{nf}}}{\beta_{T_f}} \\ &= G_r \frac{(\rho_{nf} \beta_{T_{nf}})}{(\rho_f \beta_{T_f})} \left(\frac{\rho_f}{\rho_{nf}} \right) = G_r A_4 A_1. \end{aligned}$$

Similarly, using (2.9), the model (2.7) becomes:

$$\begin{aligned} &\frac{\partial(\theta(T_w - T_\infty) + T_\infty)}{\partial(\mu_0 \bar{t}/(\rho_f u_0^2))} + w_0(u) \frac{\partial[\theta(T_w - T_\infty) + T_\infty]}{\partial(\mu_0 \bar{y}/(\rho_f u_0))} \\ &= \frac{1}{(\rho c_p)_{nf}} \frac{\partial}{\partial(\mu_0 \bar{y}/(\rho_f u_0))} \left(A_5 \kappa_0 e^{\beta \theta} \frac{\partial(\theta(T_w - T_\infty) + T_\infty)}{\partial(\mu_0 \bar{y}/(u_0 \rho_f))} \right) \\ &+ \frac{1}{(\rho c_p)_{nf}} Q(T_w - T_\infty) \theta \end{aligned}$$

⇒

$$\begin{aligned} &\frac{(T_w - T_\infty) u_0^2 \rho_f}{\mu_0} \frac{\partial \theta}{\partial \bar{t}} + \frac{w_0(u) (T_w - T_\infty) u_0 \rho_f}{\mu_0} \frac{\partial \theta}{\partial \bar{y}} \\ &= \frac{\kappa_0}{(\rho c_p)_{nf}} \frac{u_0^2 \rho_f^2}{\mu_0^2} (T_w - T_\infty) \frac{\partial}{\partial \bar{y}} \left(A_5 \rho^{\beta \theta} \frac{\partial \theta}{\partial \bar{y}} \right) \\ &+ \frac{Q}{(\rho c_p)_{nf}} (T_w - T_\infty) \theta. \end{aligned}$$

⇒

$$\begin{aligned} \frac{\partial \theta}{\partial \bar{t}} + \frac{w_0(u)}{u_0} \frac{\partial \theta}{\partial \bar{y}} &= \frac{\kappa_0}{(\rho c_p)_{nf}} \frac{\rho_f}{\mu_0} \frac{\partial}{\partial \bar{y}} \left(A_5 e^{\beta \theta} \frac{\partial \theta}{\partial \bar{y}} \right) + \frac{Q \mu_0}{u_0^2 \rho_f (\rho c_p)_{nf}} \theta \\ &= \frac{A_2}{P_r} \frac{\partial}{\partial \bar{y}} \left(A_5 e^{\beta \theta} \frac{\partial \theta}{\partial \bar{y}} \right) + Q_s \theta. \end{aligned}$$

Because

1.

$$\frac{\kappa_0}{(\rho c_p)_{nf}} \frac{\rho_f}{\mu_0} = \frac{\kappa_0 \rho_f}{\mu_0 (\rho c_p)_{nf}} \frac{c_{p,f}}{c_{p,f}} = \frac{\kappa_0}{\mu_0 (c_{p,f})} \frac{(\rho c_p)_f}{(\rho c_p)_{nf}} = \frac{A_2}{P_r}.$$

2.

$$Q_s = \frac{Q \mu_0}{(U_0^2 \rho_f (\rho c_p)_{nf})}.$$

2.2 Summary

Dropping the bars, we have arrived at the following nondimensional equations:

$$\frac{\partial u}{\partial t} + \lambda e^{-\gamma u} \frac{\partial u}{\partial y} = \frac{A_1}{(1 - \phi)^{2.5}} \frac{\partial}{\partial y} \left(e^{-\alpha \theta} \frac{\partial u}{\partial y} \right) - A_1 A_3 H^2 u + A_1 A_4 G_r \theta, \quad (2.10)$$

$$\frac{\partial \theta}{\partial t} + \lambda e^{-\gamma u} \frac{\partial \theta}{\partial y} = \frac{A_2}{P_r} \frac{\partial}{\partial y} \left(A_5 e^{\beta \theta} \frac{\partial \theta}{\partial y} \right) + Q_s \theta, \quad (2.11)$$

subject to the conditions

$$\begin{aligned} u(0, t) &= 0, \quad u(1, t) = e^t \quad \text{for all } t \geq 0, \\ \theta(0, t) &= \theta(1, t) = 0.5, \quad \text{for all } t \geq 0, \\ u(y, 0) &= y^2, \quad \theta(y, 0) = 0.5 \quad \text{for all } y \in [0, 1], \end{aligned} \quad (2.12)$$

where $\lambda, \alpha = \bar{\alpha}(T - T_\infty), \beta = \bar{\beta}(T - T_\infty), \phi, n_p$ are the wall suction parameter, viscosity reduction parameter, thermal conductivity parameter, nanoparticle's volume fraction, and shape factor respectively. The constants, $A_1 - A_5$, in (2.10) and (2.11) are also dimensionless and are defined through the thermo-physical quantities as follows:

$$\begin{aligned} A_1 &= \frac{\rho_f}{\rho_{nf}} = \frac{\rho_f}{[(1-\phi)\rho_f + \phi\rho_s]}, \quad A_2 = \frac{(\rho C_p)_f}{(\rho C_p)_{nf}} = \frac{(\rho C_p)_f}{[(1-\phi)(\rho c_p)_f + \phi(\rho C_p)_p]}, \\ A_3 &= \frac{\sigma_{nf}}{\sigma_f} = \frac{3\left(\frac{\sigma_p}{\sigma_f} - 1\right)\phi}{\left(\frac{\sigma_p}{\sigma_f} + 2\right) - \left(\frac{\sigma_p}{\sigma_f} - 1\right)\phi}, \quad A_4 = \frac{(\rho\beta^*)_{nf}}{(\rho\beta^*)_f} = (1-\phi) + \phi\frac{(\rho\beta^*)_s}{(\rho\beta^*)_f}, \\ A_5 &= \frac{\kappa_{nf}}{\kappa_f} = \frac{\kappa_p + (n_p)\kappa_0 - (n_p - 1)\phi(\kappa_0 - \kappa_p)}{\kappa_p + (n_p - 1)\kappa_0 + \phi(\kappa_0 - \kappa_p)}. \end{aligned} \quad (2.13)$$

3 Numerical Scheme and Analysis

We now formulate a finite difference approximation of the model formulated in (2.10)-(2.12). To this end let $N_y > 1$ be a positive integer representing the number of sub-intervals $[y_i, y_{i+1}]$, $i = 0, 1, 2, \dots, N_y$ in $[0, 1]$ where $y_i = ih, h = 1/N_y$. Hence, we have the mesh

$$\Omega_h = \{y_i | y_i = ih, i = 0, 1, \dots, N_y\}.$$

Choose Δt and N_t such that N_t is a positive integer. Then we discretize time interval, $t^n := n\Delta t$ for $n = 0, 1, \dots, N_t$.

Our goal is to find the following approximations of the solution at the grid points:

$$u_i^n \approx u(y_i, t^n) \text{ and } \theta_i^n \approx \theta(y_i, t^n).$$

Define the grid functions,

$$a(u_i^n) = \lambda e^{-\gamma u_i^n}, \quad \Gamma_i^n = \frac{A_1}{(1-\phi)^{2.5}} e^{-\alpha \theta_i^n}, \quad \Psi_i^n = \frac{A_2 A_5}{P_r} e^{\beta \theta_i^n} \quad (3.1)$$

and the intermediate values:

$$\Gamma_{i\pm 1/2}^n = \frac{\Gamma_i^n + \Gamma_{i\pm 1}^n}{2}, \quad \Psi_{i\pm 1/2}^n = \frac{\Psi_i^n + \Psi_{i\pm 1}^n}{2}. \quad (3.2)$$

Since $a(u) = \lambda e^{-\gamma u}$ is non-negative, we adopt the upwind approximation, [25-30] for the suction term. By adopting backward Euler time integration and "freezing" nonlinear coefficients [14, 21, 31], we arrive at the following finite difference approximation:

Velocity Scheme

$$\begin{aligned} u_i^{n+1} &= u_i^n - \Delta t \frac{u_i^{n+1} - w_{i-1}^{n+1}}{h} a(u_i^n) \\ &+ \frac{\Delta t}{h^2} \left(\Gamma_{i-1/2}^n (u_{i-1}^{n+1} - u_i^{n+1}) + \Gamma_{i+1/2}^n (u_{i+1}^{n+1} - u_i^{n+1}) \right) \\ &+ \Delta t \left(-A_1 A_3 H^2 u_i^{n+1} + A_1 A_4 G_r \theta_i^n \right) \quad \forall (i, n). \end{aligned} \quad (3.3)$$

Temperature Scheme

$$\begin{aligned} \theta_i^{n+1} = & \theta_i^n - \Delta t \frac{\theta_i^{n+1} - \theta_{i-1}^{n+1}}{h} a(u_i^n) \\ & + \frac{\Delta t}{h^2} \left(\Psi_{i-1/2}^n (\theta_{i-1}^{n+1} - \theta_i^{n+1}) + \Psi_{i+1/2}^n (\theta_{i+1}^{n+1} - \theta_i^{n+1}) \right) \\ & + \Delta t Q_s \theta_i^{n+1} \quad \forall (i, n). \end{aligned} \quad (3.4)$$

Subject the following initial and boundary conditions:

$$\begin{aligned} u_i^0 = & y_i^2, \quad \theta_i^0 = 0.5, \quad \forall y_i \in \Omega_h, \\ u_0^{n+1} = & 0, \quad u_{N_y}^{n+1} = e^{-t^{n+1}}, \quad \theta_0^{n+1} = \theta_{N_y}^{n+1} = 0.5 \quad \forall n. \end{aligned} \quad (3.5)$$

It is easy to show that the scheme proposed in (3.3)-(3.5) satisfies the positivity condition which guarantees monotocity of the algorithm [31, 32]. The formulation follows the algorithm implemented in *parabolicSolver* which is an in-house code developed by the first author and has been widely verified for convergence, see [22, 23] using the method of manufactured solutions [34, 35].

4 Results

The scheme formulated in the previous section is implemented in *parabolicSolver*, a C++ code developed by the first author and has been validated for accuracy and convergence in several studies, see [14–16, 29, 31] for example. Except otherwise stated, the following data values are used to obtain the results; $P_r = 0.7$, $G_r = 1.0$, $G_s = 0.05$, $H = 1.0$, $\lambda = 0.5$, $\gamma = 1.0$, $\alpha = 1.0$, $\beta = 1.0$, $\phi = 0.1$, $n_p = 3.0$ (spherical shape). The values of the thermo-physical properties are displayed in Table 1, see [1, 11]:

Table 1: Thermo-physical Properties

| Property | Water | Copper |
|----------------|---------------------|-----------------------|
| $\rho(kg/m^3)$ | 997.1 | 8933 |
| $C_p(J/kgK)$ | 4179 | 385 |
| $\kappa(W/mK)$ | 0.613 | 400 |
| $\sigma(S/m)$ | 0.05 | 5.96×10^7 |
| $\beta^*(1/K)$ | 21×10^{-5} | 1.67×10^{-5} |

Finally, the numerical solutions are computed on a grid with 50 grid points in $[0, 1]$, with time step size of 0.005 and the solution is outputted after $t = 10$. The influence of changing the values of the various parameters on the velocity and temperature profiles are shown in Figures 2-8. In particular, the parameters of interest are the shape factor and volume fraction of copper nonaparticles. Others are the viscosity, thermal conductivity and suction parameters.

Figure 2 displays the velocity profiles for different values of viscosity parameter, α . It is seen that the higher the values of this parameter, the higher the velocity of the fluid. This is because increasing the values of β would decrease the fluid viscosity given by $u_{nf} = \frac{\mu_0 e^{-\beta\theta}}{(1-\phi)^{2.5}}$ (in nondimensional form). Hence, the decrease in viscosity causes the flow to increase.

Figure 3 shows the plot of the velocity distribution for various values of the suction parameter, λ . One can observe that increasing the values of λ leads to decrease in the velocity. This is also physically realistic because suction is a form of flow towards the lateral direction which is perpendicular to the main flow which is along the channel axis (x -axis). Hence, the perpendicular flow would cause a decrease in the main flow, leading to a decrease in the velocity u .

Figure 4 displays the velocity profiles for different values of volume fraction of the copper nanoparticles. It shows that an increase in the volume fraction causes a decrease on the velocity of the nanofluid. This is due to the fact that more mass is being added into the fluid which increases the nanofluid density. This then decreases the flow.

The influences of the thermal conductivity and suction parameters on the temperature are depicted graphically in Figures 5 and 6. It can be seen that increasing the thermal conductivity parameter leads to a decrease in the nanofluid temperature while increasing the suction parameter only leads to very slight change in the temperature.

The impact of copper nanoparticle shape on the nanofluid is displayed in Figure 7. It can be seen that the particles with shape factor of 3 lead to increased temperature more than the others. This means that spherical shaped copper nanoparticles enhance the temperature more than cylindrical or brick shaped copper nanoparticles.

Finally, the influence of the volume fraction of copper nanoparticles on water-copper nanofluid is displayed in Figure 8. It can be seen that increasing the copper nanoparticle volume fraction ϕ increases the temperature. This is because the addition of more nanoparticles increases the thermal boundary layer [11], hence enhances the thermal conductivity.

4.1 Velocity Variations

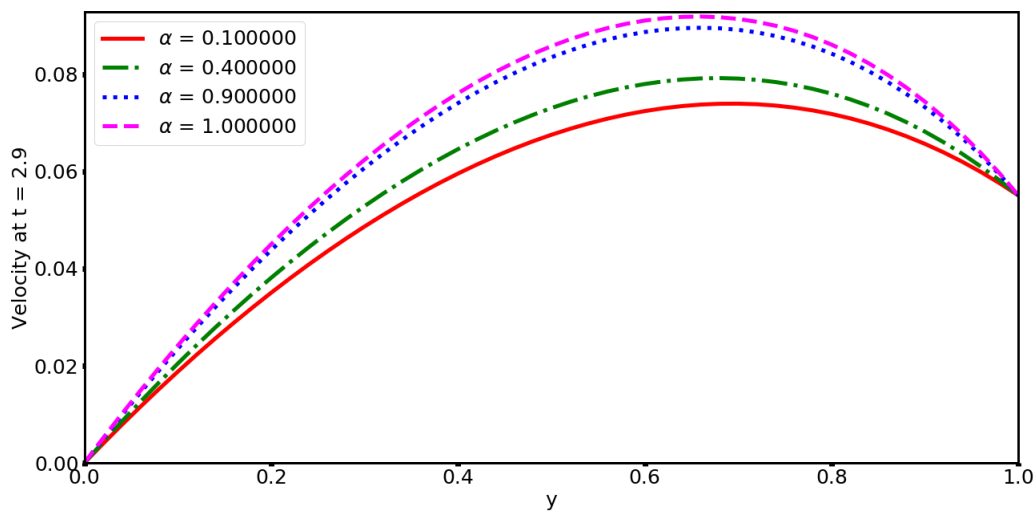


Figure 2: Velocity Variations with change in Viscosity Parameter, α

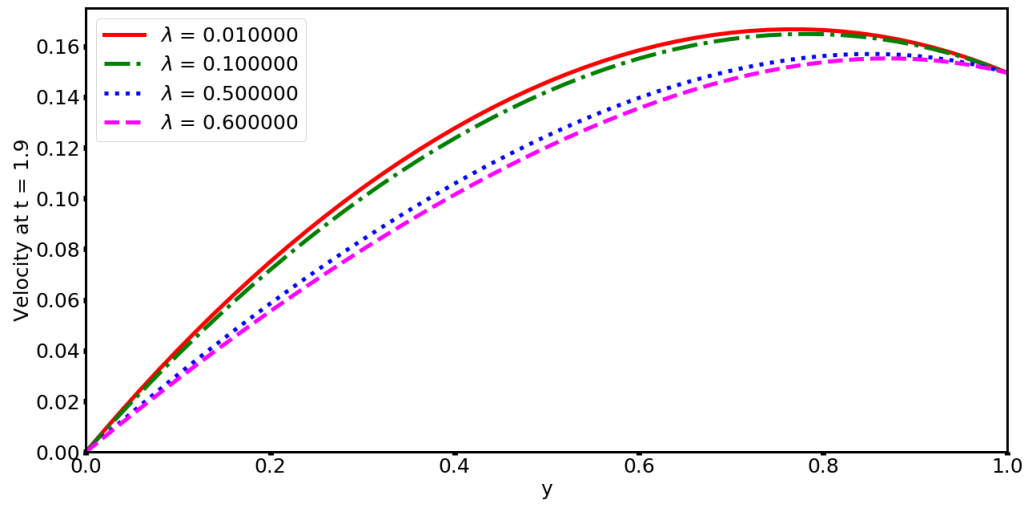


Figure 3: Velocity Variations with change in Suction Parameter, λ

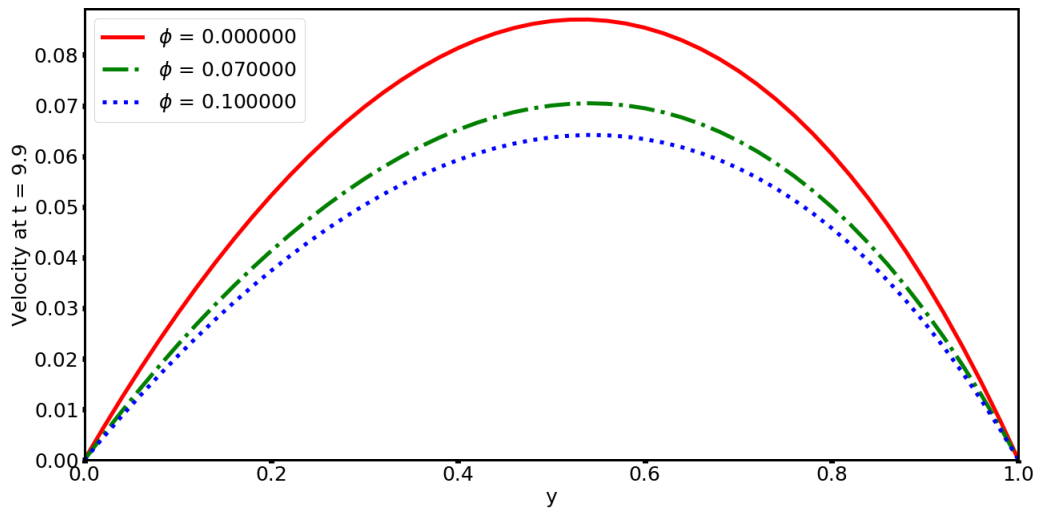


Figure 4: Effect of Nanoparticle Volume Fraction, ϕ , on the Velocity profile

4.2 Temperature Variations

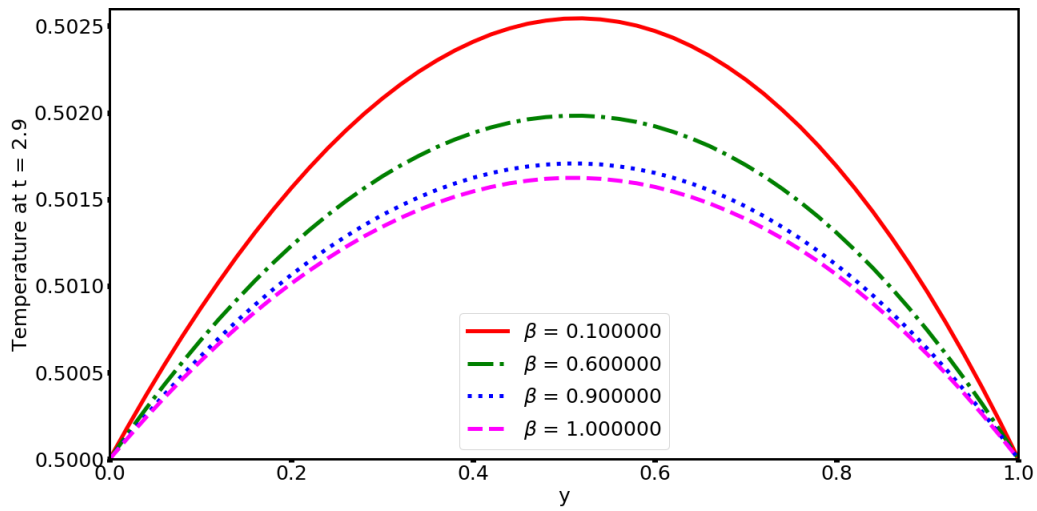


Figure 5: Effect of Thermal Conductivity Parameter, β , on the Temperature profile

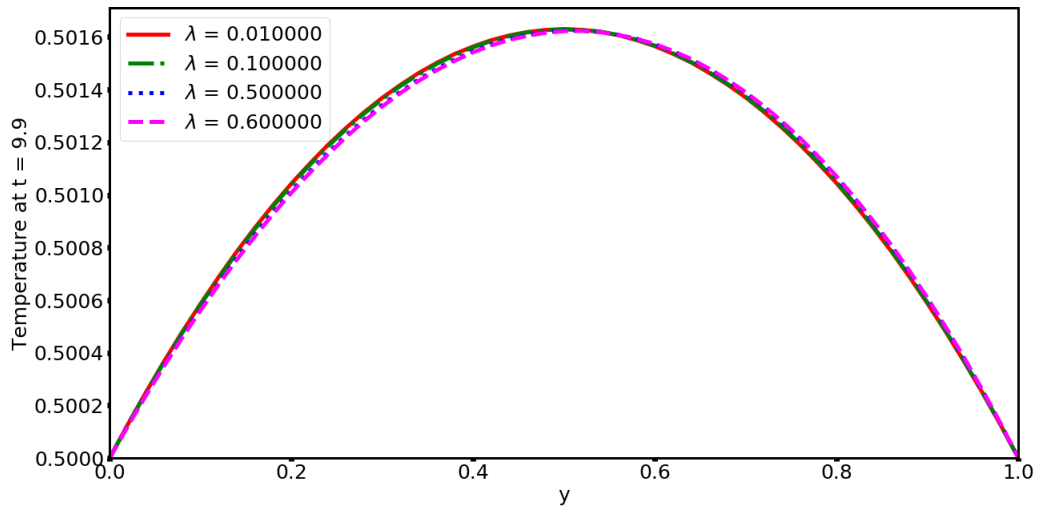


Figure 6: Effect of Suction Parameter, λ , on the Temperature profile

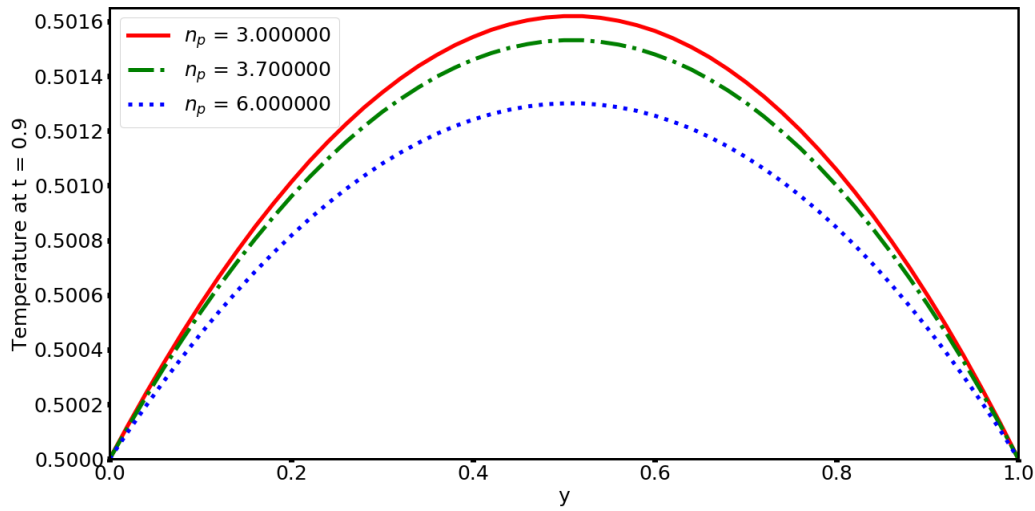


Figure 7: Effect of Nanoparticle's Shape, n_p , on the Temperature profile

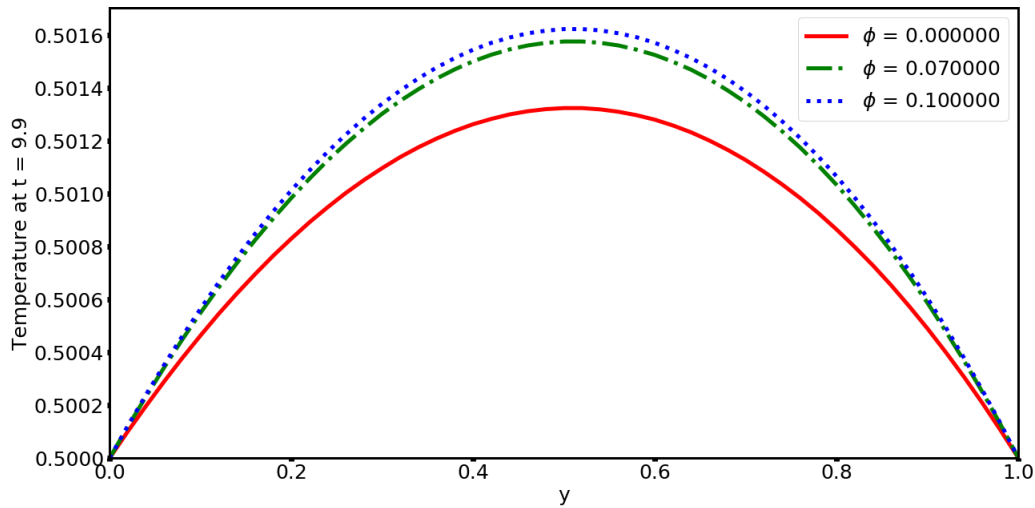


Figure 8: Effect of Nanoparticle Volume Fraction, ϕ , on the Temperature profile

5 Conclusion

The flow of water-copper nanofluid in a rectangular channel has been investigated with temperature-dependent thermophysical properties accounted for. The influence of the volume fraction and shape of nanoparticles, the variable viscosity, thermal conductivity, and suction parameters on the flow are investigated. The results show that

1. increasing the volume fraction decreases the velocity but increases the temperature,
2. copper nanoparticles of spherical shape lead to enhanced temperature than other shapes, and
3. increasing the viscosity parameter increases the flow.

It is our suggestion that more investigation be carried out to incorporate the effect of viscous dissipation, and cross-diffusion on the flow, also the effects on skin friction and Nusselt should be studied.

References

- [1] T. Hayat, B. Ahmed, F. Abbasi, and A. Alsaedi. Hydromagnetic peristalsis of water based nanofluids with temperature dependent viscosity: a comparative study. *Journal of Molecular Liquids*, 234, 324–329, (2017).
- [2] S. U. Choi and J. A. Eastman. Enhancing thermal conductivity of fluids with nanoparticles. *Technical report, Argonne National Lab.(ANL), Argonne, IL (United States)*, (1995).
- [3] K. Khanafer, K. Vafai, and M. Lightstone. Buoyancy-driven heat transfer enhancement in a two-dimensional enclosure utilizing nanofluids. *International journal of heat and mass transfer*, 46(19), 3639–3653, (2003).
- [4] A. A. Alrashed, O. A. Akbari, A. Heydari, D. Toghraie, M. Zarringhalam, G. A. S. Shabani, A. R. Seifi, and M. Goodarzi. The numerical modeling of water/fmwcnt nanofluid flow and heat transfer in a backward-facing contracting channel. *Physica B: Condensed Matter*, 537, 176–183, (2018).
- [5] M. Jafaryar, M. Sheikholeslami, and Z. Li. Cu-water nanofluid flow and heat transfer in a heat exchanger tube with twisted tape turbulator. *Powder technology*, 336, 131–143, (2018).
- [6] R. U. Haq, S. Nadeem, Z. Khan, and N. Noor. Mhd squeezed flow of water functionalized metallic nanoparticles over a sensor surface. *Physica E: Low-dimensional Systems and Nanostructures*, 73, 45–53, (2015).
- [7] K. K. Asogwa, F. Mebarek-Oudina, and I. Animasaun. Comparative investigation of water-based Al_2O_3 nanoparticles through water-based CuO nanoparticles over an exponentially accelerated radiative rigid plate surface via heat transport. *Arabian Journal for Science and Engineering*, 47(7), 8721–8738, (2022).
- [8] M. Turkyilmazoglu. Nanofluid flow and heat transfer due to a rotating disk. *Computers & Fluids*, 94, 139–146, (2014).
- [9] T. Hayat, M. Imtiaz, and A. Alsaedi. Impact of magnetohydrodynamics in bidirectional flow of nanofluid subject to second order slip velocity and homogeneous/heterogeneous reactions. *Journal of magnetism and magnetic materials*, 395, 294–302, (2015).
- [10] A. Kasaeian, R. Daneshzarian, O. Mahian, L. Kolsi, A. J. Chamkha, S. Wongwises, and I. Pop. Nanofluid flow and heat transfer in porous media: a review of the latest developments. *International Journal of Heat and Mass Transfer*, 107, 778–791, (2017).
- [11] W. Abbas and M. Magdy. Heat and mass transfer analysis of nanofluid flow based on Cu, Al_2O_3 , and TiO_2 over a moving rotating plate and impact of various nanoparticle shapes. *Mathematical Problems in Engineering*, 2020, 1–12, (2020).
- [12] M. Heydari and H. Shokouhmand. Numerical study on the effects of variable properties and nanoparticle diameter on nanofluid flow and heat transfer through micro-annulus. *International Journal of Numerical Methods for Heat & Fluid Flow*, (2017).
- [13] F. M. Abbasi, T. Hayat, S. A. Shehzad, F. Alsaadi, and N. Altoaibi. Hydromagnetic peristaltic transport of copper-water nanofluid with temperature-dependent effective viscosity. *Particology*, 27, 133–140, (2016).

- [14] C. Nwaigwe, A. Weli, and O. D. Makinde. Computational analysis of porous channel flow with cross-diffusion. *American Journal of Computational and Applied Mathematics*, 9(5), 119–132, (2019).
- [15] C. Nwaigwe. Analysis and application of a convergent difference scheme to nonlinear transport in a brinkman flow. *International Journal of Numerical Methods for Heat & Fluid Flow*, 30(10), 4453–4473, (2020).
- [16] C. Nwaigwe, J. Oahimire, and A. Weli. Numerical approximation of convective brinkman-forchheimer flow with variable permeability. *Applied and Computational Mechanics*, 17(1), (2023).
- [17] H. C. Brinkman. The viscosity of concentrated suspensions and solutions. *The Journal of chemical physics*, 20(4), 571–571, (1952).
- [18] S. Srinivas, R. Gayathri, and M. Kothandapani. Mixed convective heat and mass transfer in an asymmetric channel with peristalsis. *Communications in Nonlinear Science and Numerical Simulation*, 16(4), 1845–1862, (2011).
- [19] V. Narla, K. Prasad, and J. Ramanamurthy. Peristaltic transport of jeffrey nanofluid in curved channels. *Procedia Engineering*, 127, 869– 876, (2015).
- [20] R. L. Hamilton and O. Crosser. Thermal conductivity of heterogeneous two-component systems. *Industrial & Engineering chemistry fundamentals*, 1(3), 187–191, (1962).
- [21] C. Nwaigwe. Mathematical modeling and numerical analyses of transport phenomena with variable cross-diffusion and nonlinear radiation. *Computational Thermal Sciences: An International Journal*, 13(1), (2021).
- [22] C. Nwaigwe and O. D. Makinde. Finite difference investigation of a polluted non-isothermal non-newtonian porous media flow. *Diffusion Foundations*, 26(4), 145–156, (2019).
- [23] C. Nwaigwe, R. Ndu, and A. Weli. Wall motion effects on channel flow with temperature-dependent transport properties. *Applied Mathematics*, 9(3), 162–168, (2019).
- [24] A. Weli and C. Nwaigwe. Numerical analysis of channel flow with velocity-dependent suction and nonlinear heat source. *Journal of Interdisciplinary Mathematics*, 23(5), 987–1008, (2020).
- [25] R. J. Leveque. *Numerical Methods for Conservation Laws*. Birkhauser verlag, (1992).
- [26] R. J. Leveque. *Finite volume methods for hyperbolic problems*. Cambridge university press, 31, (2002).
- [27] C. Nwaigwe and C. Orji. Second-order non-oscillatory scheme for simulating a pressure-driven flow. *Journal of the Nigerian Association of Mathematical Physics*, 52(1), 53–58, (2019).
- [28] C. Nwaigwe and A. Weli. Analysis of two finite difference schemes for a channel flow problem. *Asian Research Journal of Mathematics*, 15, 1–14, (2019).
- [29] E. F. Toro. *Riemann solvers and numerical methods for fluid dynamics: a practical introduction*. Springer Science & Business Media, (1999).
- [30] E. F. Toro. *Shock Capturing Methods For Free-surface Flows*. Wiley, (2001).
- [31] C. Nwaigwe. An unconditionally stable scheme for two-dimensional convection-diffusion-reaction equations. https://www.researchgate.net/publication/357606287_An_Unconditionally_Stable_Scheme_for_Two-Dimensional_Convection-Diffusion-Reaction_Equations, (2022). (Accessed on 19-January-2023).



- [32] P. Matus, F. Gaspar, V. T. K. Tuyen, et al. Monotone difference schemes for weakly coupled elliptic and parabolic systems. *Computational Methods in Applied Mathematics*, 17(2), 287–298, (2017).
- [33] P. Matus, L. G. Vulkov, et al. Analysis of second order difference schemes on non-uniform grids for quasilinear parabolic equations. *Journal of Computational and Applied Mathematics*, 310, 186–199, (2017).
- [34] C. Nwaigwe and A. Weli. Ishikawa-collocation method for nonlinear fredholm equations with non-separable kernels. *Journal of Advances in Mathematics and Computer Science*, 38(3), 1–11, (2023).
- [35] A. Weli and C. Nwaigwe. Computational analysis of two numerical solvers for functional fredholm equations. *International Journal of Mathematical and Computational Methods*, 8, 1–8, (2023).